1-1-2006

Towards improving positioning accuracy of conducting polymer actuators

Gursel Alici
University of Wollongong, gursel@uow.edu.au

Nam N. Huynh
University of Wollongong, nhuynh@uow.edu.au

Towards Improving Positioning Accuracy of Conducting Polymer Actuators

Gürsel ALICI and Nam N. HUYNH
School of Mechanical, Materials and Mechatronic Engineering
University of Wollongong
2522, NSW, Australia

Abstract – Recently, there have been significant developments in conducting polymers, particularly in their synthesis and use as electromechanical actuators. This is mainly due to their many promising features including biocompatibility, high force to weight ratio, suitability to open loop control. On the other hand, they suffer from nonlinear problems such as hysteresis and creep. With this in mind, it is the aim of this study to evaluate the existence level of these nonlinearities and their mathematical modeling in order to improve the positioning accuracy of conducting polymer actuators. The polymer actuator considered in this study which has a symmetrical structure can operate in both liquid and non-liquid media as opposed to its predecessor. The actuator drives a rigid link, like positioning a payload. The experimental results demonstrate that while the hysteresis is negligibly small, the level of the creep is significant enough to model it and subsequently employ the model to improve steady-state positioning of the actuator. Based on experimental results, a viscoeleastic model is employed to describe the creep behaviour. The outcomes of this study will pave the way towards understanding of the limitations as well as potential usefulness of conducting polymer actuators in many cutting edge applications ranging from biomedical to micro/nano manipulation systems.

Keywords – electroactive polymer actuators, creep, hysteresis, motion control, micro/nano manipulation.

I. INTRODUCTION

Conducting polymer actuators have attracted the attention of many researchers in the last decade [1-8] as potential electromechanical actuators and sensors, which are very suitable to miniaturization. A comprehensive account of polymer actuators is given in [6, 9]. They have a composite structure with polymer layers separated from each other with an insulator causing volume expansion and contraction. When the right stimulus, which is usually a very small voltage –typically 1V, or a current, is applied to the polymer layers, a volume expansion and contraction occurs as a result of electrochemical doping and undoping of ions. The change in the volume generates a bending displacement -- the electrochemical energy is converted into mechanical energy. As a result, a considerable amount of research has been devoted to modeling and understanding their behaviours in order to improve their synthesis conditions such that they can be reliable actuators and sensors for new cutting applications ranging from biomedical devices to micromanipulators [4,7,10]. Zhou et al. [4] have reported on three types of polymer actuators including ionic conducting polymer film actuator, polyaniline actuator, and parylene thermal actuator. They have presented their fabrication and initial performance results. Smela et al. [7] have presented the development and performance outcomes of PPy and Au bilayer conducting polymer actuators operating in electrolyte solutions. As an extension of this study, Jager et al. [10] has fabricated a serially connected micromanipulator to pick, move, and place 100μm glass beads. It has been demonstrated that the micromanipulator is very suitable for single-cell manipulation. The application of conducting polymer actuators is an emerging field as researchers begin to harness the benefits of their material properties, which are greatly enhanced at smaller scales [9, 22]. Possible future applications include artificial muscles, and a wide variety of sensors and actuators in biomedical systems [6] and micro/nano manipulation systems [11,15]. As these actuators do not contain any rolling and sliding elements, they can be suitable to micro/nano manipulation tasks, which require motion accuracy in the order of 0.05 to 0.1 micrometer (50 to 100 nanometer). We have established a two-finger robotic gripper articulated with bending-type conducting polymer actuators [16]. The gripper with the dimensions of 10 mm x 1mm x 0.17mm can lift an object as much as 50 times the actuator weight.

We have previously reported [12-15] on developing various mathematical models to predict the bending behaviour of the conducting polymer actuators and employing the models to optimize their geometry leading to high force and displacement outputs. In this study, we report on evaluating the nonlinear behaviour of conducting polymer actuators and proposing ways of compensating nonlinearities in order to improve their positioning accuracy. The conducting polymer actuator considered is like a cantilevered beam bending under the influence of an internally induced bending moment while carrying a rigid link. We have experimentally demonstrated that while the hysteresis is negligibly small, the creep can cause significant positioning errors if it is not compensated. On the other hand, Otero and Cortes [21] have reported that once the applied potential is stopped, the movement of the tri-layer polymer actuator working in an aqueous electrolyte remains constant. Further, it has been stated that unless "the electrical conditions are unchanged, the position of the triple layer remains fixed." However, our experimental investigation

into a triple layer polymer actuator operating in air (non-aqueous) shows that there is non negligible creep in the position of the actuator when a full oxidation is reached without changing the electrical conditions, i.e. applying a constant potential continuously. Further, the actuator relaxes back to its neutral position once the applied potential is switched off.

II. STRUCTURE OF POLYMER ACTUATOR

The cross section of the bending type polymer actuator considered in this study is shown in Fig. 1. The outmost two layers are polypyrrole (PPy) with thicknesses of 30 μm. The middle layer is polyvinylidine fluoride (PVDF), an inert, non conductive, porous polymer serving as the separator of two electroactive PPy layers and reservoir for electrolyte $TBA.PF_6$ (tetrabutylammonium hexafluorophosphate) 0.05 M in solvent propylene carbonate. Thin layers of platinum of 10 to 100 Å are sputtered on the top of PVDF to enhance the conductivity between PPy layers and electrolyte.

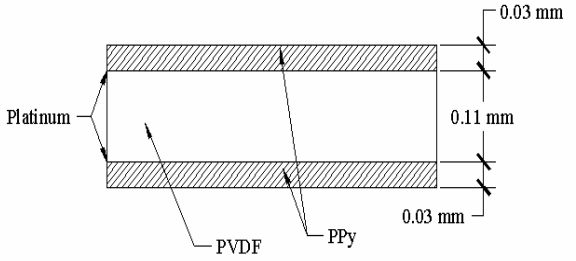

Figure 1. Cross section of the PPy-based actuator (not to scale)

The structure of the actuator driving a rigid link – a finger of a robotic gripper-- is shown in Fig. 2.

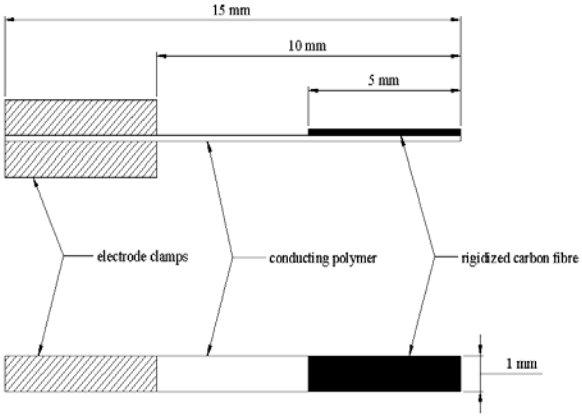

Figure 2. Structure and dimensions of the robotic finger (front view and top view).

The finger is basically a strip of PPy-based conducting polymer loaded by a thin layer of rigid carbon fibre, in which the conducting polymer works as *an actuator and a joint* while the carbon fibre attached on the top of the polymer serves as a rigid link for the robotic finger. The finger is typically 1 mm wide, 10 mm long (5 mm for actuator part and 5 mm for rigid part).

The fabrication process of the robotic finger is briefly outlined as follows.

- The sheet of conducting polymer is trimmed into strips of 1x15 mm^2 and carbon fibre is trimmed into pieces of 1x5 mm^2.
- Carbon fibre pieces are cured in an oven for about 10 minutes at 100°C. Carbon fibre should be very rigid after taken out of the oven.
- Double-sided sticky tape is placed onto rigid carbon fibre pieces.
- The rigid carbon fibre piece with the sticky tape on one side is then attached to the polymer strip.

The samples are replenished in tetrabutylammonium hexaflourophosphate ($TBA.PF_6$) 0.05 M electrolyte for five minutes before each test.

III. EXPERIMENTAL METHOD

The schematic representation of the experimental setup is shown in Fig. 3.

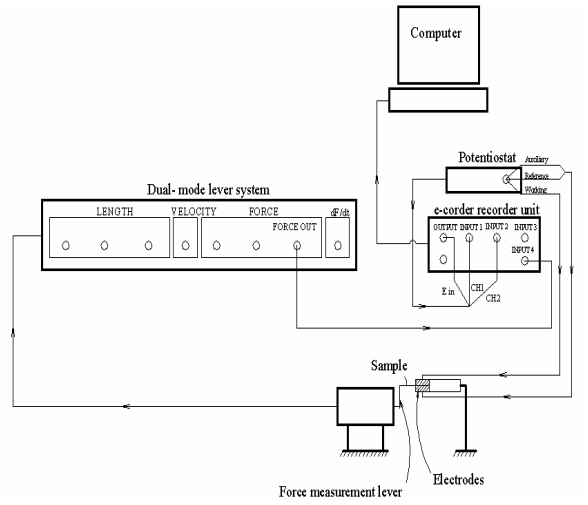

Figure 3. Schematic representation of the equipment setup.

As shown by the arrows in Fig. 3, the input voltage from potentiostat is applied to an actuator sample via the electrode clamps. The movement of the polymer strip under applied voltage is recorded using a digital camera and a grid paper. The input current and voltage are sent directly from potentiostat to the e-corder recorder unit and are also displayed on the computer screen. For the creep tests, step input voltages of 0.2 V, 0.4 V, 0.6 V, 0.8 V and 1.0 V were applied. The results presented here are for the robotic finger set to move in the horizontal plane in order to exclude any influence of the gravitational force from the creep measurements. Preliminary experiments, however, showed that tests running in horizontal plan and vertical plan give relatively similar results, which means the effect of external force due to weight of carbon fiber to the creep behavior of the robotic finger is negligible.

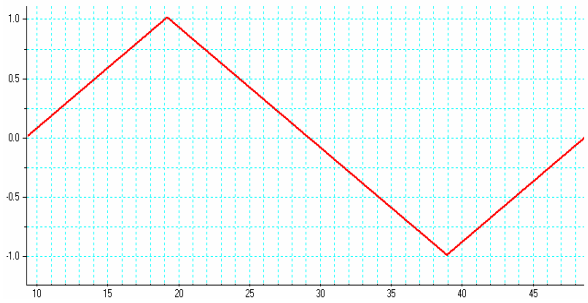

Figure 4. The form of the input voltage used in hysteresis experiments.

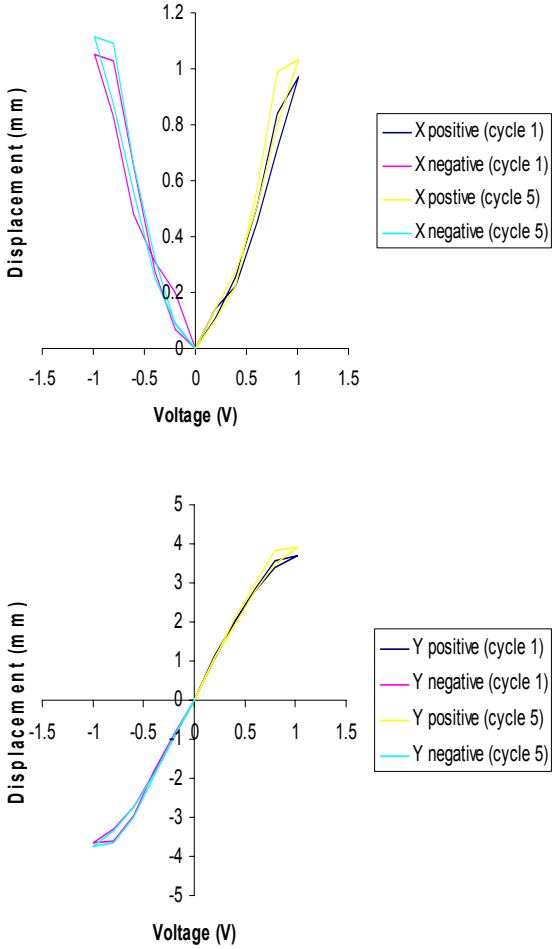

Figure 5. The X and Y displacements of the robotic finger under a ±1V cyclic triangle input.

IV. HYSTERESIS RESULTS

Samples for this experiment are as shown in Fig. 2 or in Fig.7. The input voltage in the form of a cyclic triangle signal, as shown in Fig. 4, is applied to the actuator sample driving the rigid link. The movement of the actuator sample is recorded after one cycle and five working cycles by a digital video camera. The result is provided in Fig.5. The tip position of the robotic finger is defined by X, Y coordinates of the tip and bending angle θ, as shown in Fig. 6. The origin is fixed at the finger tip. X axis directs towards the root of the strip and Y axis directs towards the side of the strip where carbon fiber is attached.

With reference to the results shown in Fig.5, the level of the hyteresis is not significant. The output current versus the output voltage curve, known as a voltammetry diagram, which is recorded for the same sample to verify whether the hysteresis is significant is shown in Fig.7. The upper and lower portions of the voltammetry diagram are known as the oxidation and reduction curves, respectively. If the curves are symmetrical about the horizontal zero axis, this will indicate no hysteresis [20]. The symmetry is evident in Figure 7. However, it was reported in the literature [7] that there exists significant hysteresis (27º of the bending angle) in bilayer polymer (polypyrrole) actuators operating in an aqueous electrolyte. It was suggested to use current control rather than potential control to completely eliminate the hysteresis. The mechanism behind the reported hysteresis was suggested to be due to the polymeric chain rearrangement (i.e. transitions between benzoid and quinoid structures taking place during oxidation and reduction processes) during the movement of ions in and out of the polymer layer [20].

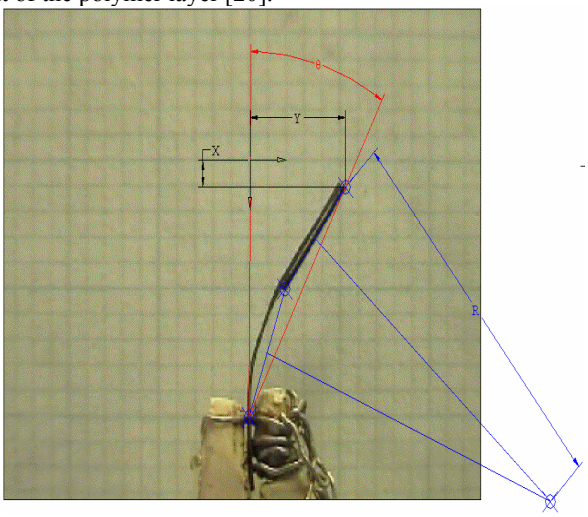

Figure 6. Demonstration of parameters defining the strip position: coordinate systems, bending angle and radius.

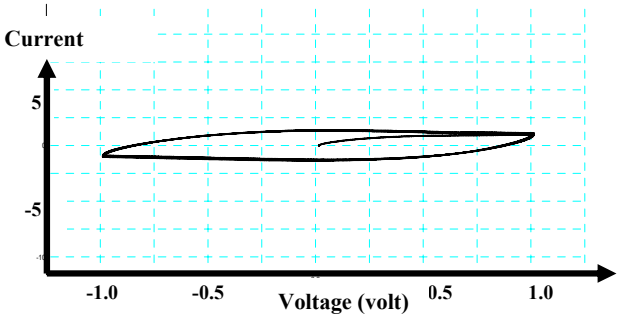

Figure 7. The voltammetry diagram for the hysteresis results shown in Fig. 5. It is recorded for the first 5 cycles.

V. CREEP RESULTS

We describe the creep behaviour in conducting polymer actuators as the change in the tip position of the actuator after the polymer layers are fully oxidized or reduced, i.e. – a zero current output is recorded from the polymer layers. The creep observed for a 0.6V input is presented in Fig. 8. With reference to the coordinate frame described in Fig.6, the tip positions are identified as the robotic finger continuously bends under the effect of step input voltages ranging from 0.2V to 1.0 V. Tip coordinates X, Y and bending angle θ for five cases of input voltages are plotted against time, as shown in Figs. 9 – 11.

The vertical lines across response curves of 0.2 V, 0.4 V and 0.6 V in Figs. 9-11 indicate the point where the creep starts. Zero current could not be obtained during the experiment period for input voltages of 0.8 V and 1.0 V, and hence, the creep response in these cases could not be observed. The data, however, can be used to verify the theoretical creep model

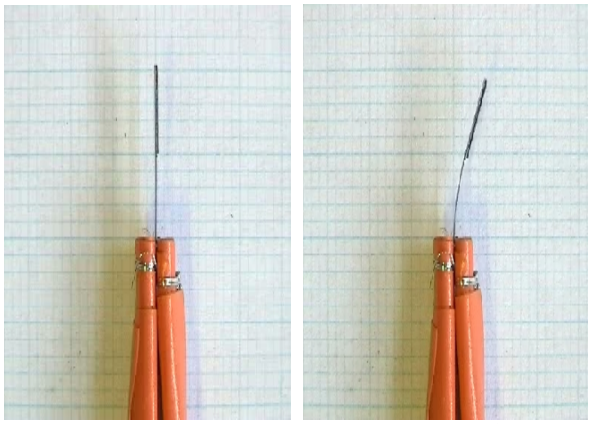

t = 0 s

t = 275 s (Creep starts)

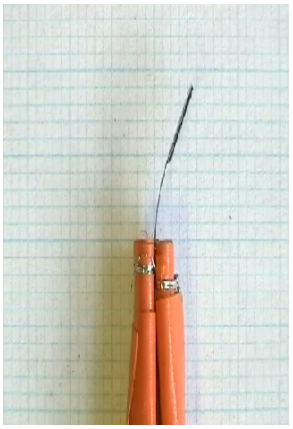

t = 1800 s (Test ends)

Figure 8. Photos of robotic finger at creep starting point and end of test point for input voltage of 0.6V.

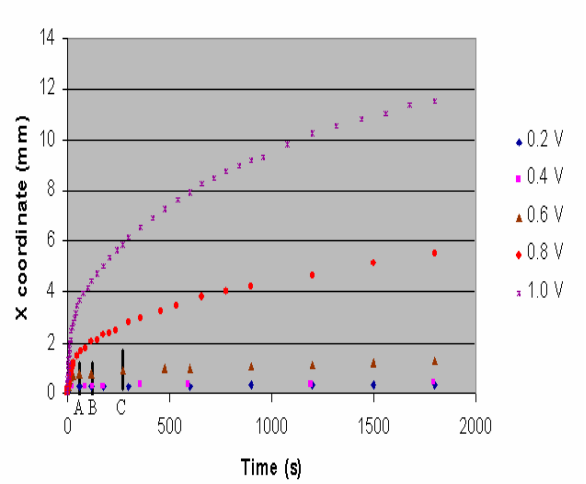

Figure 9. X coordinate of tip displacement versus time. Creep starts at A, B and C for input voltages of 0.2 V, 0.4 V and 0.6 V, respectively.

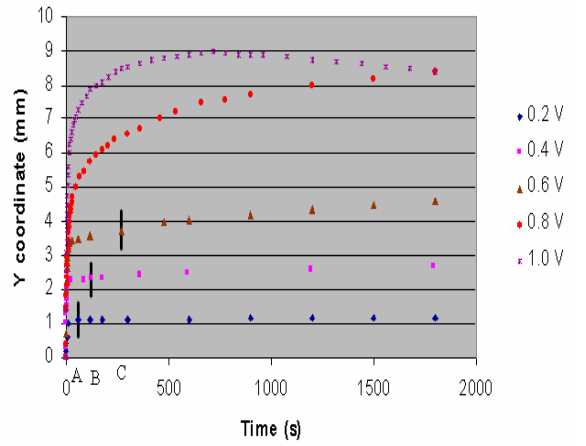

Figure 10. Y coordinate of tip displacement versus time. Creep starts at A, B and C for input voltages of 0.2 V, 0.4 V and 0.6 V, respectively.

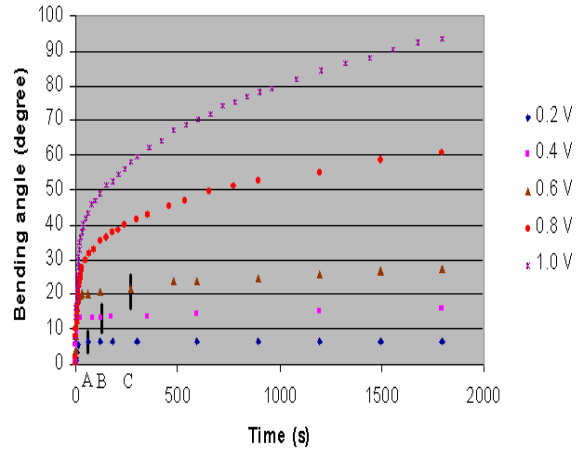

Figure 11. Bending angle θ versus time. Creep starts at A, B and C for input voltages of 0.2 V, 0.4 V and 0.6 V, respectively.

VI. VISCOELASTIC MODEL

The low-frequency creep response of the robotic finger can be represented by a system of spring and damper elements, known as Kelvin-Voigt viscoeleastic model

shown in Fig.12. This model was originally proposed to mimic the viscoeleastic behaviour of polymers [17] and later that of piezoactuators, [18], [19].

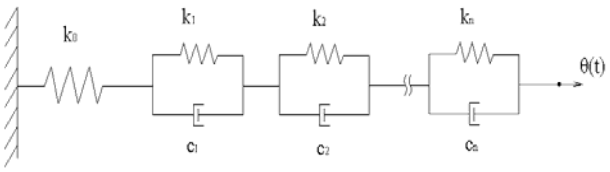

Figure 12. Kelvin-Voigt model for viscoelastic materials.

The transfer function representation of this model is given by

$$\frac{\theta(t)}{u(t)} = \frac{1}{k_{x_0}} + \sum_{i=1}^{n} \frac{1}{k_i}\left[1 - e^{-\frac{t}{c_i/k_i}}\right] \qquad (5)$$

where θ(t) and u(t) are the bending angle and the input voltage, respectively. The first term on the right hand side represents elastic behaviour while second term, which represents Kelvin-Voigt elements, models creep behavior. The more Kelvin-Voigt elements are used in the model, the smaller is the errors between the estimated and experimental data points. The accuracy of the model is evaluated using Root Mean Square (RMS) error described by (6), and is provided in Table 1 for various number of Kelvin-Voigt elements. As expected, the higher is the order of the model, the better is fitness of the model.

$$RMS_{bending\ angle} = \sqrt{\frac{1}{N}\sum_{i=1}^{N}\left(\theta_m - \theta_e\right)_i^2} \qquad (6)$$

TABLE I.
THE RMS OF ESTIMATION ERRORS FOR VARIOUS MODELS UNDER A RANGE OF INPUT VOLTAGE.

Voltage	1st Order	2nd Order	3rd Order
0.2 V	0.2154	0.0483	0.0479
0.4 V	0.7394	0.5415	0.1227
0.6 V	1.9318	0.3004	0.2078
0.8 V	5.1842	1.1743	0.4380
1.0 V	56.6855	1.4814	0.6268

The numerical values of the spring and damping parameters in (5) have been estimated for the input voltages of 0.2 V, 0.4 V, 0.6 V, 0.8 V and 1.0 V using a least-square estimation algorithm. The estimated and experimental bending angle data points are shown in Fig.13. The experimental data is the same as the data shown in Fig.11. The numerical values of the model parameters for a five-element model are provided in Table 2. It must be noted that as the creep is input dependent, it is needed to estimate the model parameters for different input voltages.

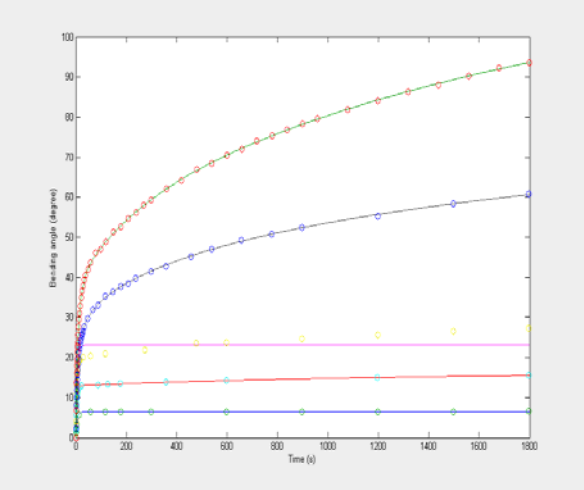

Figure 13. Experimental data points and modeling results of bending angle versus time.

TABLE II.
COEFFICIENTS OF A 5Th ORDER CREEP MODEL FOR RANGE OF INPUT VOLTAGES.

Coeff.	0.2 V	0.4 V	0.6 V	0.8 V	1.0 V
k_0	0.3791	57.257	0.3233	149.72	33.02
k_1	0.1703	0.1376	0.1410	0.0236	0.0924
c_1	0.8274	0.3874	0.7340	47.481	0.0579
k_2	0.1703	0.1076	0.141	0.1132	0.0492
c_2	0.8274	0.5554	0.734	4.7451	0.5125
k_3	0.1703	0.1315	0.141	0.0509	0.1293
c_3	0.8274	0.4967	0.734	0.5188	3.0732
k_4	0.1703	0.1218	0.141	0.0744	0.0155
c_4	0.8274	0.0883	0.734	21.348	29.441
k_5	0.1703	0.1198	0.141	0.113	0.0656
c_5	0.8274	149.82	0.734	0.0937	15.209

It has been found that the creep in the horizontal and vertical planes is quite similar. This follows that the rigid carbon fibre, which can be treated as a point mass at the tip of the actuator, does not have any apparent effect on the creep behavior. The mechanism behind the creep behaviour reported in this study can be due to the high pressure in the oxidized PPy layer. Please note that after the current through electrodes becomes to zero, the polymer is in a fully oxidized state, as described by the following chemical reaction

$$\underset{(oxidized\ state)}{PPy^{+}PF_6^{-}} + e^{-} \xleftarrow[reduction]{oxidation} \underset{(reduced\ state)}{PPy^{0}} + PF_6^{-}$$

In that PPy layer, the anions PF_6^- and solvent molecules are highly concentrated. Under this pressure, these cations and molecules can not go back to the other PPy layer as the input potential is still applied. Hence, they tend to spread around under the pressure, which results in further bending of the fully reduced PPy layer and hence generating what we call as creep. Future work involves using an ionic electrolyte with larger molecule diameter such that the cations and solvent molecules do not spread around. Our initial experimental results, which

will be reported in another publication, support this explanation.

Baughman postulated [9] that there could be 'positional drift' in conducting polymer actuators due to "electrical self-discharge or intra-electrode dopant re-distribution after a fast mechanical response". With this in mind, it was suggested to employ either feedback control of the applied potential or mechanical stops. In fact, our future research plans, (i) using an inverse viscoeleastic model to compensate for the drift or establishing a closed-loop control system based on the position data provided by a laser displacement sensor, (ii) fabricating a mechanically constrained bending actuator to prevent undesired movement under any applied voltage, revolve around those postulated suggestions.

VI. CONCLUSIONS

We have presented our experimental investigation into quantifying the hysteresis and creep behaviours of a polyprrole conducting polymer actuator driving a load in order to develop a position compensation strategy to improve the positioning accuracy of the actuator. The experimental results prove that the creep can cause significant positioning accuracy if not properly identified and compensated. The higher is the amplitude of the input voltage, the more significant is the creep. The hysterisis effect is found to be negligibly small – thanks to the symmetrical structure of the actuator. As polymers exhibit visco-elastic behaviour, Kelvin-Voigt creep model is employed to mimic the creep behaviour. Immediate future study includes developing and implementing a position control system which adjusts the voltage applied to compensate for positioning inaccuracy. As part of this aim, the Kelvin-Voigt model should also be improved to predict the creep behavior of a loaded actuator as a function of both time and input voltage.

ACKNOWLEDGEMENTS

This project has been partly funded by a URC Small Grant. The authors would like to thank Prof. Dr. G.M. Spinks, and Mr. Yanzhe (Richard) Wu from the Intelligent Polymer Research Institute for providing the actuators, allowing us to use their research facilities, more importantly sharing their sterling expertise with us.

REFERENCES

1. E. W. H. Jager, E. Smela, O. Inganas, and I. Lundstrom, "Polypyrrole Microactuators", Synthetic Metals, pp. 1309 – 1310, 1999.
2. G. M. Spinks, B. Xi, D. Zhou, V. T. Truong, and G. G. Wallace, "Enhanced control and stability of polypyrrole electromechanical actuators", Synthetic Metals, Vol.140, pp. 273 – 280, 2004.
3. J. Ding, L. Liu, G. M. Spinks, D. Zhou, V. T. Truong, G. G. Wallace, and J. Gillespie, "High performance conducting polymer actuators utilising a tubular geometry and helical wire interconnects", Synthetic Metals, Vol.138, pp. 391 -- 398, 2002.
4. J. W. L. Zhou, H. Y. Chan, T. K. H. To, K. W. C. Lai, and W. L. Li, "Polymer MEMS actuators for underwater micromanipulation", IEEE/ASME Trans. on Mechatronics, Vol.9, No.2, pp. 334 – 342, June 2004.
5. J. D. Madden, R. A. Cush, T. S. Kanigan, and I. W. Hunter, "Fast contracting polypyrrole actuators", Synthetic Metals, 113, pp. 185 – 192, 2000.
6. E. Smela, "Conjugated Polymer Actuators for Biomedical Applications", Advanced Materials, Vol.15, No.6, pp. 481 – 494, March 2003.
7. E. Smela, M. Kallenbach, and Jens Holdenried, "Electrochemically Driven polypyrrole bilayers for moving and positioning bulk micromachined silicon plates", IEEE Journal of Microelectromechanical Systems, Vol.8, No.4, pp. 373 – 383, December 1999.
8. Q. Pei, and O. Inganas, "Electrochemical applications of the bending beam method: 1.Mass transport and volume changes in polypyrrole during redox", Jounral of Physical Chemistry, Vol. 96, No.25, pp. 10507-10514, 1992.
9. R. H. Baughman, "Conducting polymer artificial muscles," Synthetic Metals, vol. 78, pp. 339-353, 1996.
10. E. W. H. Jager, O. Inganas, and I. Lunstrom, "Microrobots for Micrometer-size objects in Aqueous Media: Potential tools for Single Cell Manipulation", Science, Vol.288, pp 2335 – 2338, June 30, 2000.
11. G. Alici, and B. Shirinzadeh, "Kinematics and Stiffness Analysis of a Flexure-jointed Planar Micromanipulation System for a Decoupled Compliant Motion", 2003 IEEE/RSJ International Conference on Intelligent Robots and Systems, pp. 3282 – 3287, Las Vegas, USA, October 2003.
12. G. Alici, ,B. Mui, and C. Cook, "Bending Modeling and Its Experimental Verification for Conducting Polymer Actuators Dedicated to Manipulation Applications", Sensors and Actuators A:Physical, 2006. (In print)
13. G. Alici, P. Metz, and G. M. Spinks, "A Mathematical Model to Describe Bending Mechanics of Polypyrrole (PPy) Actuators", 2005 IEEE/ASME International Conference on Advanced Intelligent Mechatronics, pp. 1029 – 1034, Monterey, USA, July 2005.
14. G. Alici, P. Metz, and G. M. Spinks, "A Methodology towards Geometry Optimisation of High Performance Polypyrrole (PPy) Actuators", J. of Smart Materials and Structures, 2006. (In Print)
15. W. John, and G. Alici, "Towards micro and nano manipulation systems: behaviour of a laminated polypyrrole (PPy) actuator driving a rigid link", 2005 IEEE/ASME International Conference on Advanced Intelligent Mechatronics, pp. 54 – 59, Monterey, USA, July 2005.
16. G. Alici, and N. N. Huynh, "A Robotic Gripper based on Conducting Polymer Actuators", The 9th International Workshop on Advanced Motion Control, pp., Istanbul, Turkey, March 2006.
17. L.E. Malvern, *Introduction to the Mechanics of a Continuous Medium*, Prentice-Hall, Englewood Cliffs, NJ, 1969.
18. D. Croft, G. Shed, S. Devasia, "Creep, Hysteresis, and Vibration Compensation for Piezoactuators: Atomic Force Microscopiy Application", *Journal of Dynamic Systems, Measurement, and Control*, pp. 35-43, vol. 123, 2001.
19. R. Changhai, S. Lining, "Hysteresis and creep compensation for piezoelectric actuator in open-loop operation", *Sensors and Actuators A*, pp. 124-130, vol. 122, 2005.
20. G. Grande, and T. F. Otero, "Intrinsic asymmetry, hysteresis, and conformational relaxation during redox switching in polypyrrole: a coulovoltametric study", Journal of Physical Chemistry, vol.102, pp. 7535 -- 7540, 1998.
21. T. F. Otero, and M. T. Cortes, "Characterisation of triple layers," in Proc. SPIE Smart Structures and Materials: Electroactive Polymer Actuators and Devices, vol. 4329, pp. 93-100, 2001.
22. M. Roemer, T. Kurzenknabe, E. Oesterschulze, and N. Nicoloso, "Microactuators based on conducting polymers", Analytical and Bioanalytical Chemistry, Vol. 373, No.8, pp. 754-757, 2002.